Muon production: past, present and future

G H Eaton[1] and S H Kilcoyne[2]

[1]ISIS Facility, Rutherford Appleton Laboratory, England
[2]University of St Andrews, Scotland

1 The discovery of the pion and muon

The very first evidence for the existence of the muon was provided by Kunze (1933) in a Wilson cloud chamber exposed to cosmic rays. In his original photograph, shown in Figure 1, the paths of an electron and of a considerably stronger ionising particle of smaller curvature can be clearly seen. However, at that time the nature of the second particle was unknown, since it ionised too little for a proton and too much for an electron. Kunze suggested the particle was the product of a nuclear explosion, yet failed to claim the discovery of a new elementary particle.

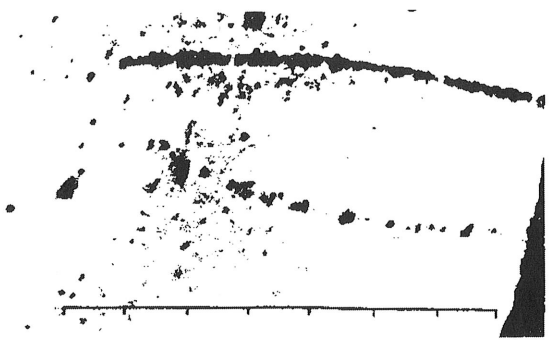

Figure 1. *The first observed muon by Paul Kunze in Rostock (1933): "Double track as a result of a probable nuclear explosion. Lower track: electron of 37 000 000V. The nature of the upper positive particle is unknown."*

The definitive discovery of the muon occurred three years later when Neddermeyer and Anderson (1937), again using a Wilson cloud chamber, carried out measurements of the energy loss of particles occurring in cosmic ray showers in heavy materials like platinum.

Their observation of particles which penetrated the absorber more strongly than electrons led to the conclusion that these particles had unit charge with a mass greater than that of electrons but much smaller than that of protons. The initial hope was that the new particle was that responsible for the strong nuclear force proposed by Yukawa in 1935. Indeed, the new particle was observed to decay into an electron, as postulated by Yukawa to explain beta-decay. However it soon became apparent from the work of Conversi et al (1947) that the new "mesotron" appeared to have a very weak nuclear interaction with matter in contradiction to the essential predicted property of the Yukawa particle. Theoretical suggestions by Tanikawa and Sakata and Inoue (Tanikawa, et al, 1946) that the explanation of these mysteries lay in a two meson hypothesis, in which a Yukawa-type strongly interacting meson (pion) decayed to a weakly interacting mesotron, were finally verified experimentally by Powell and his collaborators in Bristol (Lattes *et al.* 1947). Using nuclear emulsions they observed a number of two meson decay events, one of which is shown in Figure 2.

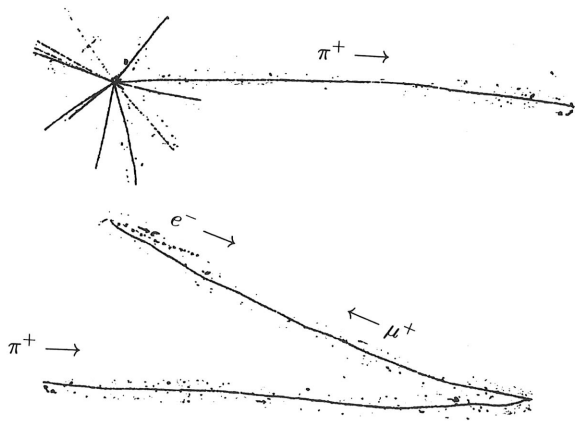

Figure 2. *Two sections of an emulsion exposure showing a two meson event. The track of the positively charged pion is emitted from a cosmic ray induced nuclear interaction (top). The continuation of the same track is shown below: the pion (from left to right) decays into a muon which moves right to left and after 600 microns travel, decays itself into a positron.*

All of the observed events displayed a constant range for the secondary muon of about 600 microns in the emulsion, leading to the conclusion that a two-body decay of the primary meson, called the π^+ or pion, to a secondary meson, μ or muon and one neutral particle was responsible. Twenty such events enabled estimates of 260±30 and 205±30 electron masses for the pion and muon mass respectively, and an estimate of approximately 10^{-8} seconds for the pion lifetime. This research verified that muons were indeed born from the decay of the pion, the particle responsible for the strong force in nuclei. It was also evident that the muon was a quite unique particle. It was weakly interacting with properties similar to those of the electron, yet almost two hundred times heavier, and with either positive or negative charge and a lifetime of a few microseconds. It is understandable that many physicists of the time including Rabi and Gell-Mann and Rosenbaum did not readily welcome the new particle as in many respects it heralded the end of innocence in their understanding of particle physics (Wu and Hughes 1977, Scheck

1978). Aspects of the fundamental muon physics will be discussed in the chapter in this volume by Jungmann. Here it simply remains to be said that many of the properties of the muon are still not fully understood.

All of the experiments described above were carried out with muons produced by cosmic rays. Major advances in muon science and its application followed from the first production of pions and muons by particle accelerators in the late 1950s. Almost all current research uses accelerator-based muon facilities, with the second generation facilities now following the early accelerators, and third generation sources on the drawing board.

2 Pion production

In the Yukawa model, the nuclear force which binds nuclei together can be described by the exchange of a quantum from one nucleon, which is immediately absorbed by another. Because the nuclear force is of extremely short range ($\sim 10^{-15}$m), the mass of the exchanged quantum or pion has to be of the order of 200 electron masses. An isolated stationary nucleon cannot emit or absorb a pion and conserve energy and momentum in the process. However, according to the Heisenberg Uncertainty Principle energy conservation can be violated by an amount ΔE for a time Δt providing $\Delta E \cdot \Delta t \sim \hbar$. If ΔE is comparable to the pion mass of ~140MeV, then Δt has to be of the order of $4{\times}10^{-24}$s, during which time the pion can travel a distance of $\hbar/mc$. In this way one can picture a nucleon as being surrounded by a virtual cloud of pions, giving a characteristic charge distribution of rms radius 0.8fm and magnetic moment of +2.79 nuclear magnetons. In order to produce pions external to the nucleon itself nucleons must be bombarded with other nucleons of sufficient kinetic energy such that the available centre of mass energy is greater than the pion mass of 140MeV. Typical nucleon-nucleon reactions producing pions are as follows,

$$\begin{aligned} p+p &\rightarrow p+n+\pi^+ \\ &\rightarrow p+p+\pi^0 \end{aligned} \qquad \begin{aligned} p+n &\rightarrow p+n+\pi^0 \\ &\rightarrow p+p+\pi^- \\ &\rightarrow n+n+\pi^+ \end{aligned} \qquad p+p \rightarrow d+\pi^+$$

These are termed single pion production reactions and have an energy threshold of approximately 280MeV in the laboratory frame. However the probability (or cross sections) for producing pions in such reactions increases rapidly with energy, as shown in Figure 3 (Guzhavin *et al.* 1964, Alexander *et al.* 1967).

To obtain a maximum number of single pions the incident protons should have energies in the range 500MeV to 1000MeV energy range (the so-called intermediate energy range). This defines the optimal energy for an accelerator-based pion (and muon) source.

The reactions listed above, which result in a final configuration of three particles (eg $pn\pi$) produce a broad distribution of pion energies, typically peaked at ~200MeV for incident protons of 600MeV. In contrast, the two body production process, $p{+}p \rightarrow d{+}\pi^+$, gives a monoenergetic pion beam of 300MeV at forward angles for the same proton energy. The cross section for this reaction as a function of proton energy is shown in Figure 4. Typical energy spectra of pions produced by various energy protons incident on carbon are shown in Figure 5.

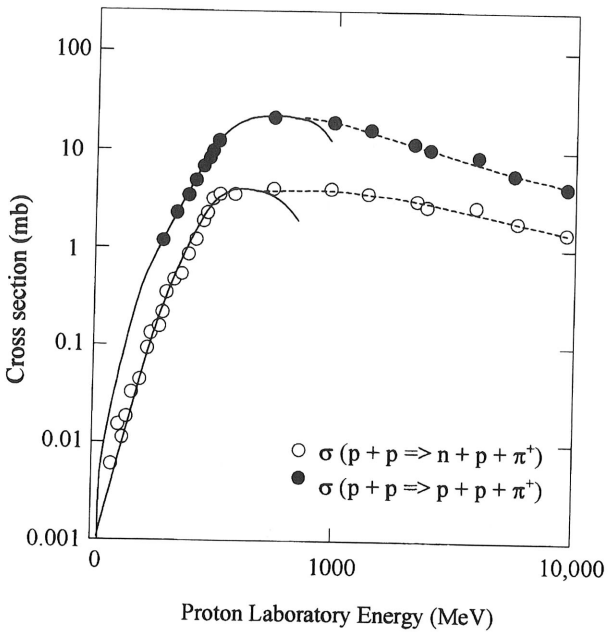

Figure 3. *Cross-sections for single pion production.*

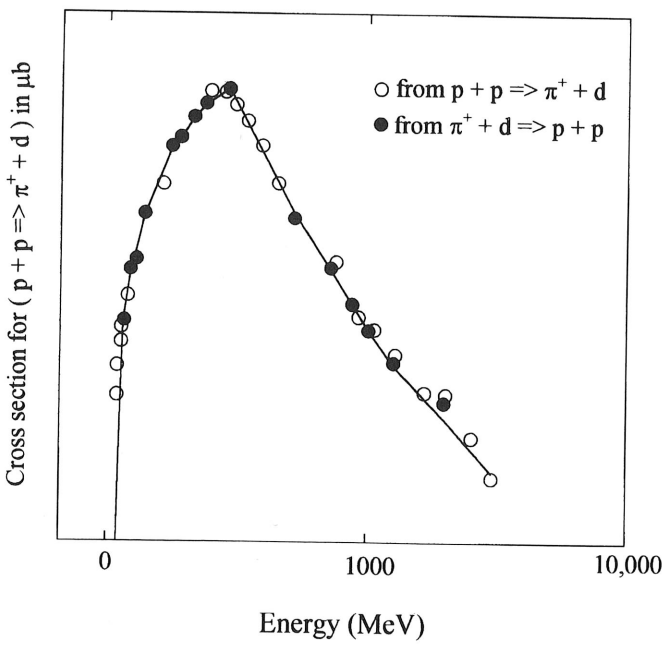

Figure 4. *Cross-section for the reaction $p + p+ \rightarrow \pi^+ + d$ including data obtained from the reverse reaction, assuming detailed balance.*

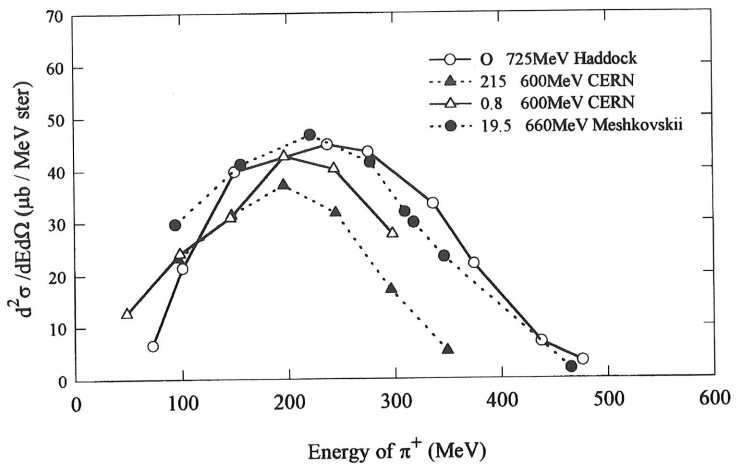

Figure 5. *Energy Spectra of π^+ produced in proton-carbon collisions.*

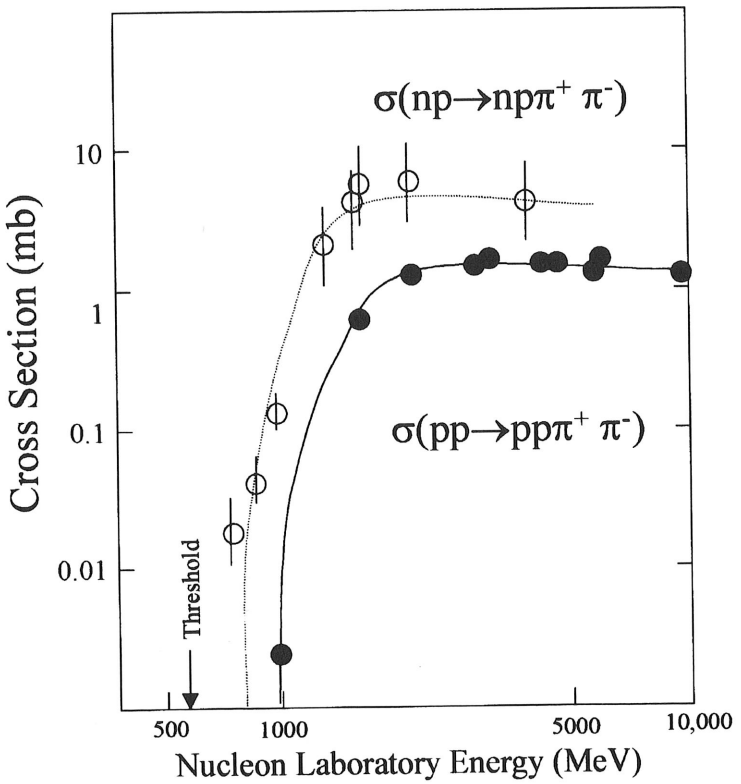

Figure 6. *Examples of cross-sections for double pion production.*

At higher energies it is possible to produce pions in pairs in the reactions given below; the double pion production cross sections are shown in Figure 6 (Alexander *et al.* 1969),

$$\begin{aligned} p+p \rightarrow\ & p+p+\pi^+ +\pi^- \\ \rightarrow\ & p+p+\pi^0+\pi^0 \\ \rightarrow\ & n+n+\pi^+ +\pi^+ \\ \rightarrow\ & n+p+\pi^+ +\pi^0 \\ \rightarrow\ & d+\pi^+ +\pi^0 \end{aligned} \qquad \begin{aligned} p+n \rightarrow\ & p+n+\pi^+ +\pi^- \\ \rightarrow\ & p+n+\pi^0+\pi^0 \\ \rightarrow\ & n+n+\pi^+ +\pi^0 \\ \rightarrow\ & p+p+\pi^- +\pi^0 \\ \rightarrow\ & d+\pi^- +\pi^+ \\ \rightarrow\ & d+\pi^0+\pi^0 \end{aligned}$$

Each of these reactions has a threshold kinetic energy in the laboratory frame of 600MeV, with the cross sections reaching saturation levels above 1.5–2.0GeV. Future accelerator based muon sources will most probably be in this energy regime and benefit substantially from double pion contributions to the pion and hence to the muon production rates.

3 Properties of the pion and pion decay

The properties of the pions are summarised below.

Charge States	π^+	π^-	π^0
Mean life (s)	26.04×10^{-9}	26.04×10^{-9}	0.89×10^{-16}
Spin	0	0	0
Mass (MeV)	139.5679	139.5679	134.97
Decay modes	$\pi^+ \rightarrow \mu^+ + \nu_\mu$ (weak decay)	$\pi^- \rightarrow \mu^- + \bar{\nu}_\mu$	$\pi^0 \rightarrow \gamma + \gamma$

Pion decay modes other than those shown in the table are negligible at the 10^{-4} level. The two decay process of a charged pion (139.5679MeV) into a muon (105.65946MeV) (Particle Data Group 1978) and a supposed massless neutrino, results in a unique energy and momentum (4.1MeV and 29.7877MeV/c) for the muon emerging from the reaction if the parent pion is at rest. A precise measurement of the muon momentum from this decay process provides, to date, the best available upper limit for the muon neutrino mass (Daum *et al.* 1979). The zero spin of the pion is deduced from the lack of fine structure in π-mesic x-rays (Carrigan 1968).

For muon neutrinos the half integer spin and momentum are antiparallel (ie the neutrino has a left handed spin with helicity of –1), while for antineutrinos the spin and momentum are parallel (ie the antineutrino has a right handed spin with helicity +1). The fact that neutrinos emitted in $\pi+$ decay can only have a negative helicity is a direct result of parity violation in the weak interaction. In the decay process at rest $\pi^+ \rightarrow \mu^+ + \nu_\mu$, the muon and neutrino have opposite momenta (to conserve momentum), so that it follows that the muon and neutrino must have anti parallel spins to conserve angular momentum in the decay. The muons produced in pion decay at rest are emitted isotropically in space. Because the decay process is via the weak interaction (and hence parity violating), the neutrino spin s_ν is in the opposite direction to its momentum p_ν. Since the pion has zero spin, the muon must have its spin opposite to its propagation direction. Hence the muons emitted in any chosen direction must be 100% polarised (all spinning in the same direction), a crucial requirement for their use in μSR.

4 Muon sources

4.1 Surface and decay muons

The first generation of proton accelerators capable of providing intense beams of pions and hence muons, became available towards the end of the 1950s. With these accelerators great advances in muon research were achieved and the embryonic sciences of muon spin rotation (μSR), muon catalysed nuclear fusion (μCF) and fundamental particle physics with muons were born. These early accelerators , notably the Nevis Columbia, SREL Berkeley USA and CERN Synchrocyclotrons, were followed in 1974 by the second generation meson factories at Los Alamos, SIN (PSI) Zurich Switzerland and TRIUMF Vancouver. These muon sources, which are more than two orders of magnitude more intense, have enabled muon science to become firmly established. These continuous (or more strictly quasi-continuous) sources were followed in 1981 by the pulsed facility (BOOM) in Japan, and finally in 1987 by the worlds most intense pulsed facility at ISIS at the Rutherford Appleton Laboratory in the UK. The following table shows a compilation of these first and second generation accelerators.

Accelerator and location	**Present energy (MeV)**	**Date of first Operation**
Sector focused cyclotrons		
Univ of Maryland, USA	140(p)	1968
TRIUMF, Vancouver, Canada	500(H-)	1973 (?)
Sector focused ring cyclotrons		
Univ of Indiana, USA	200	1972 (?)
Zürich, Switzerland	520	1974 (?)
Proton synchrocyclotrons		
McGill Univ, Canada	100	1949
Harvard Univ, USA	160	1949
Harwell, UK	160	1949
Orsay, France	160	1958
Uppsala, Sweden	185	1951
Rochester, USA	240	1948
Liverpool, UK	380	1954
Columbia Univ, USA	385	1950
Carnegie-Mellon Univ, USA	440	1951
Chicago, USA	460	1951
CERN, Switzerland	600	1957
SREL, Newport News, USA	600	1966
Dubna, USSR	680(p)	1949
Berkeley, USA	740(p)	1946
Gatchina, USSR	1000	1968
Proton linear accelerators		
Los Alamos, USA	800	1972 (?)
Proton synchrotrons		
Birmingham, UK	1000	1953
Brookhaven, USA	3000	1952

(continued)

Saclay, France	3000	1958
Princeton, USA	3000	1963
Berkeley, USA	6200	1954
Chilton, UK	7000	1963
Moscow, USSR	7000	1961
Dubna, USSR	10000	1957
Argonne, USA	12500	1963
CERN, Switzerland	28000	1959
Brookhaven, USA	33000	1960
Serpukhov, USSR	76000	1967
Batavia, USA	200000	1972 (?)

All of the muon facilities rely upon muon beams generated by a proton beam impacting a low Z target. Low Z materials are optimal for high pion production, and also for low multiple scattering of the proton beam and hence minimal activation of the downstream proton channel. There are two ways of generating muon beams from these pions. The first and most important is to use low energy pions which come to rest in the muon target and which subsequently decay in the target. Because the resulting muons are of low energy (4.1MeV), only those with sufficient range to escape the target stop near or on the surface of the target slab. Hence these muons are known as 'surface' or 'ARIZONA' (Piper *et al.* 1976) muons and, as described before, they are 100% polarised in any chosen direction of emission from the target. Because the pion stopping density in the target is very high surface muon beams are of high intensity. Moreover, if the proton beam focus at the target is small then a small source of muons is produced. In principal this allows an equally small image to be produced at the experimental station at the end of the extracted muon beam-line.

A disadvantage of surface muon beams is that only polarised positive μ^+ muons are produced as the negative π^-, once stopped in the graphite target, are immediately captured by the carbon nuclei. For negative muons production it is necessary to utilise pions with sufficient energy to escape the production target, and direct as many as possible into a region of high longitudinal magnetic field (usually provided by a superconducting solenoid some metres in length) in which they can decay in flight. The resulting muons may subsequently be selected in momentum and transmitted to the experiment. This type of beam line, known as a 'Decay' beam and can produce both polarised μ^+ and μ^- over a wide momentum band and is generally considered the 'Rolls Royce' of muon channels, costing typically £10M compared with ~£2M for a simple surface beam. In decay channels the pion decay is considered relative to the laboratory frame of reference and both the transverse and longitudinal momentum components of the moving particles must be considered. In particular, if a cone or a cylinder of observation, with an axis coincident with the direction of both pion propagation and muon emission, is considered two specific cases can be distinguished:

- The muon is emitted in the direction of pion propagation. The momenta p_μ^0 and p_π of both particles are additive. The muon is emitted in the "forward" direction, i.e. the resultant momentum p_μ is greater than that of the pion from which it originated, and it has a spin antiparallel to p_μ .

- A muon emitted in the direction opposite to pion propagation will carry a resultant momentum p_μ smaller than p_π. Such a "backward" muon will have its spin pointing in the direction of propagation.

The recipe for obtaining polarised muons either μ^+ or μ^- from a decay channel is therefore quite simple. The momentum of muons required for the experiment is chosen and all magnets in the muon section of the beamline are set to transmit these muons. The momentum of the pions entering the superconducting solenoid is selected to correspond to that appropriate for "backward" or "forward" decay of the pions.

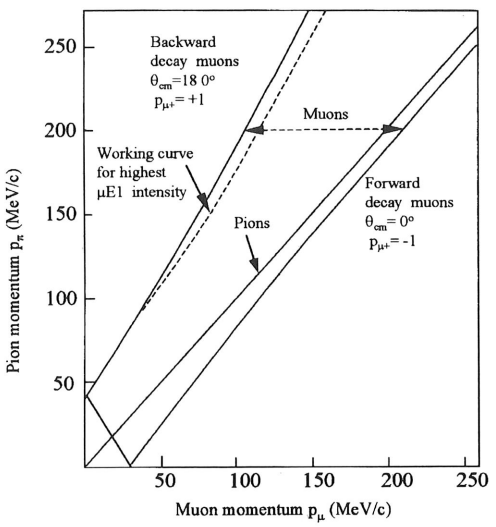

Figure 7. *Decay kinematics for pion decay in flight.*

The required information for these selection processes is shown in Figure 7, which displays the forward and backward muon momenta as a function of pion momentum (SIN Users Handbook 1981). For practical reasons, it is usual to choose "backward" decay muons. As an example, if 50MeV/c muons are required then from Figure 7 it can be seen that pions of $\sim$ 112MeV/c should be injected into the superconducting magnet decay section. Such a decay beam produces muon polarisation of 70%–80% due to the finite kinematical acceptance of the channel, which results in contamination by imperfect backward decays.

4.2 Transport of muons to the experiment

Muons are charged particles and hence can be deflected and guided in magnetic and electric fields. Quadrupole magnets are used for focusing the muon beam whilst dipole bending magnets are used to select a particular momentum bite. Electrostatic fields are used in special devices to deflect the muons either alone or in combination with magnetic fields.

The force on a non-relativistic particle of mass m, velocity v, change e, passing through a magnetic field B perpendicular to its path is given by Bev in a direction perpendicular

to B and v. The particle executes a circular path of radius R in the field such that $Bev = mv^2/R$. The deflection angle in passing through the field is proportional to Be/mv, and the necessary magnetic fields in quadrupole and bending magnets are thus proportional to the momentum, p, of the particles concerned. Similar consideration for electrostatic deflections show that the electric fields should be proportional to βp where $\beta = v/c$. In general deflecting devices based upon electrostatic fields are suitable only for low particle momenta and velocities, higher momentum particles are more efficiently deflected using magnetic fields.

The primary task of a muon beamline is to collect and transmit as many of the muons produced in the target as is possible within the typical aperture constraints of the various elements in the beam-line. If a quadrupole magnet is used as a horizontally focusing device it is, of necessity, vertically defocusing. Such magnets must be therefore be used in pairs (quadrupole doublet) or in threes (triplet) to produce a net focusing in both horizontal and vertical directions.

In pulsed muon beams such those at the ISIS facility, special care must be taken to remove contaminant particles from the beam. In a positive surface muon beam these are principally positrons arising from the decay of π^0 produced in the target and the subsequent materialisation of electron positron pairs in reactions

$$\pi^0 \rightarrow \gamma\gamma\,, \qquad \gamma \rightarrow e^+e^-$$

The resulting positrons have a velocity close to that of light (ie $\beta = 1$, in contrast to $\beta = 0.24$ for surface muons). Such positrons must be removed as they simulate muon decay with the sample. This is achieved using a cross-field electrostatic separator. At ISIS, for example, this consists of a vertical electric field between horizontally disposed electrodes, and a horizontal magnetic field generated by ancillary coils. In such a device, particles of momentum p (GeV/c) and velocity β $(= v/c)$ are deviated vertically by an angle $\Delta\theta$ (mrad) given by the expression.

$$\Delta\theta = \frac{d}{p}\left[\frac{\epsilon}{\beta} - 300B\right]$$

where d is the length in m, ϵ is the electric field gradient in MV/m, and B is the field in Tesla. For surface muons ($p = 0.0265$GeV/c, $\beta = 0.24$) it can be arranged that $\Delta\theta = 0$ when $\epsilon/\beta = 300B$, and the muons are transmitted through the device without deviation. For positrons of the same momentum, however, $\beta = 1$ and a vertical deviation occurs which is sufficient to remove them from the beam. This device essentially acts as a velocity selector. Typical values, such as those used at ISIS, of a 100kV field over a 13cm gap of the separator cancelled by a magnetic field of 10.69mT produces a vertical deviation for positrons of 92mrad.

The cross field separator also induces a rotation in the polarisation of the muon given by $\phi = eBd/\beta\gamma$ where e is the muon charge and $\gamma = 1/\sqrt{1-\beta^2}$. For an electric field of 100kV $\phi = 6.6°$ at surface momentum pointing upwards relative to the direction of travel of the muons. Given sufficient electric field gradient and length, a $\pi/2$ rotation can be achieved, providing a transformation from longitudinal to transverse polarisation. Such a capability, which requires an electric field of 454kV generated over two cross field separators each 1.5m long can provide additional flexibility in muon beam instrumentation.

It should be noted that continuous muon sources, such as those at PSI and TRIUMF, do not require a positron elimination device. At such sources a very thin plastic scintillation detector placed before the μSR sample can distinguish positrons and muons counted individually by the amount of light they generate in the detector. Positrons are 'minimum ionising' particles in such a plastic scintillator and therefore can readily be vetoed from the larger light pulse generated by the slower muon.

4.3 Muon range and range straggling within a sample

The purpose of transporting muons from the target station to the beam line is, of course, to implant them in a sample. The implantation range R of surface muons in a sample has an associated range width or straggling, ΔR, arising in part from the statistical nature of the muon energy loss processes and in part from the momentum spread of the incident muons. R and ΔR are given by the following expressions

$$\begin{aligned} R &= ap^{3.5} \\ \Delta R &= a\left[0.008 + 12.25\left(\frac{\Delta p}{p}\right)^2\right]^{1/2} p^{3.5} \end{aligned}$$

where p is the muon momentum in MeV/c. For surface muons of p=26.5MeV/c, $R\rho$ is typically 110mg/cm^2 (where ρ is the sample density) and ΔR = 20% of R. For typical samples the range is therefore between 0.1 and 1mm. The muons therefore stop in the bulk material and not at the surface. Decay beams of high momentum p, allow much longer ranges and hence the use of sample containers with thick walls, such as pressure cells, whilst on the other hand slow muons such as discussed by Morenzoni can be used to probe surfaces and near surfaces with reasonable precision. Typical values of the range and straggling are shown as a function of muon energy in the following table The last line of this table refers to surface muons.

Kinetic Energy E (keV)	**Range** R (nm)	**Straggling** ΔR (nm)
0.010	0.5	0.3
0.100	2.1	1.3
1.0	13.1	5.4
10.0	75.0	18.0
30.0	244.0	36.0
E (MeV)	R (μm)	ΔR (μm)
4	710	100

5 An example of a pulsed muon facility: ISIS

Intense beams of polarised muons are the essential prerequisite for almost all aspects of μSR science. As we shall see from other chapters in this book, the predominant demand is for spin polarised positive muons, although several research fields, such as muon catalyzed fusion, also require beams of negative muons in which the degree of polarisation is immaterial. A further consideration is that muon facilities, and hence the muon beams

themselves, may have either a continuous or a pulsed time structure. This time structure often directly influences the nature of the μSR science that is performed at the respective facility. In this remainder of this chapter we shall discuss the key elements of the world's most powerful pulsed muon facility, ISIS, although we shall also highlight the significant differences between this pulsed muon sources and the principal continuous muon sources at PSI in Switzerland (Abela *et al.* 1991) and TRIUMF in Canada (Marshall 1991). We shall also consider the future prospects for μSR science in the light of recently proposed major new international muon facilities.

5.1 The ISIS proton synchrotron and extracted proton beam

The time structure of any pulsed muon beam is dependent upon the character of the proton beam with which it is produced. In our discussion of the ISIS Pulsed Muon Facility we shall therefore begin with an overview of the proton production. A schematic diagram of the ISIS Spallation Neutron source is shown in Figure 8.

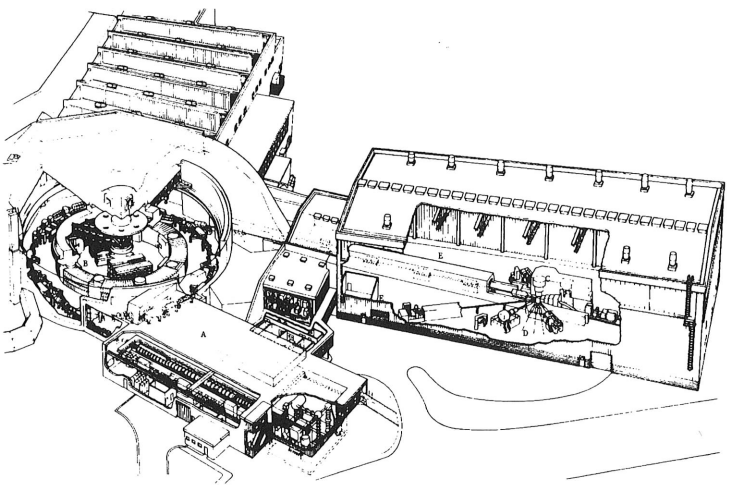

Figure 8. *Lay-out of the ISIS pulsed neutron and muon source at The Rutherford Appleton Laboratory, showing the LINAC injector, synchrotron, extracted proton beam and spallation neutron target station. The muons are generated from an intermediate target 20m upstream of the neutron target.*

The principal component of ISIS is a rapid cycling proton synchrotron which produces a high intensity 200μA (1.2×10^{15} pps) proton beam at 800MeV. This is used in conjunction with a heavy (high Z) stopping target (such as U or Ta) to create high intensity beams of pulsed neutrons by the spallation process. Indeed ISIS is currently the world's most powerful pulsed neutron source by a factor of thirty. Although ISIS produces pulses of protons at a frequency of 50Hz, the synchrotron itself operates at twice the circulation frequency of the protons resulting in a double pulsed proton beam with the time structure shown in Figure 9. This is of crucial importance for the muon facilities at ISIS, as the muon beams essentially preserve this time structure, and as a result are pulsed at 50Hz

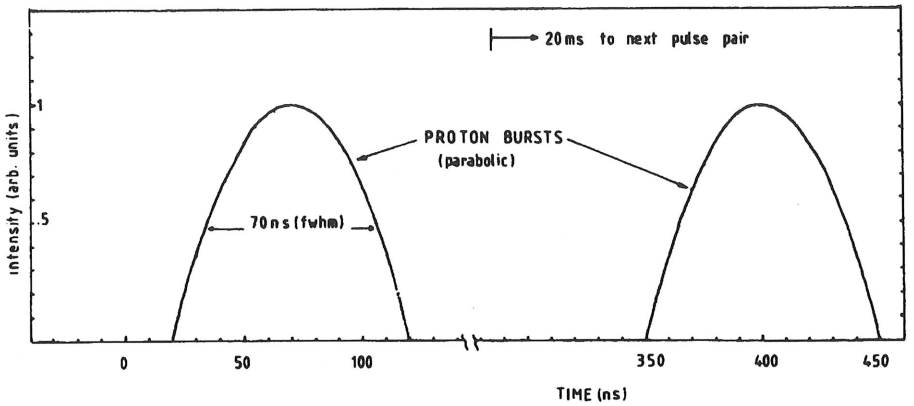

Figure 9. *Time structure of the proton bursts from the ISIS synchrotron.*

with a double pulse substructure, with each sub-pulse approximately 70ns wide (FWHM) and separated by 330ns from its partner. In contrast, the PSI and TRIUMF meson factories operate with a quasi-continuous 20ns time structure, such that muon facilities at both of these laboratories are essentially continuous. It is this intrinsic time structure of the muon pulse that defines not only the character of the muon source but also the nature of the μSR experiments which can be performed there.

5.2 The muon target station

At ISIS the muon targets are thin slabs of pyrolytic graphite (5–10mm thick in the dimension parallel to the proton beam direction). Typically 2–3% of the incident protons interact with the ISIS target; the remaining 97% passing unhindered to the neutron target station. The 10mm targets operate at 500° at a proton beam current of 200μA, and generate approximately 1kW of power. Edge cooling of these targets is therefore required. At TRIUMF similar targets are used, whilst those at PSI are radiatively cooled rotating wheels of pyrolytic graphite approximately 50mm thick. The single target at ISIS serves both the EC and the Japanese RIKEN/RAL muon facilities

5.3 The ISIS EC surface muon beam line

The general layout of the ISIS Surface Muon Beam Facility (Eaton *et al.* 1988) is shown in Figure 10. The surface muons are collected by the quadrupoles Q1, Q2 close to the target after passage through the thin aluminium window separating the vacuum systems of the muon and proton channels. These muons are momentum analysed in the magnet B1 which is set at the same integrated magnetic field as B2. Q3, Q4 and Q5 produce a dispersed focus of the beam in the middle of Q4, near to which is a horizontal collimator used to select the momentum bite of the beam. Q7, Q8 transmit the muons through the drift space Q7–Q8 in which is situated the cross field electrostatic separator A used to eliminate the positrons in the beam. The beam line is completed by a quadrupole doublet Q8, Q9 which produces a simultaneous horizontal and vertical focus of the muons at the

sample position in the μSR spectrometer situated at the end of the beam line. The muon beam line is set at a surface muon momentum of 26.5MeV/c transmitting all positively charged particles of this momentum.

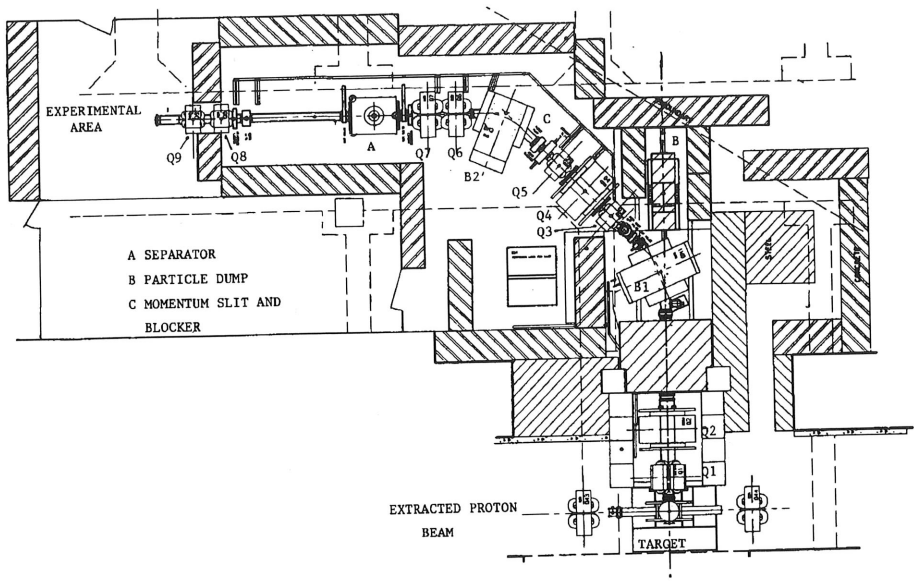

Figure 10. *Layout of the ISIS pulsed muon beam. Muons are produced in thin graphite targets located in the extracted proton beam and collected at a central production angle of 90°. A dispersed focus is produced in the centre of the Q4 quadrupole. Horizontal achromaticity is achieved after the second bending magnet. Positron separation is obtained using the 1m*

5.3.1 Muon pulse management

In order to overcome problems associated with the double pulse time structure, a fast electrostatic (E-field) kicker was initially installed in the beam line, to suppress entirely the second muon pulse (Borden *et al.* 1990). The principle, and efficiency, of this method was extended in 1993, with the creation of the European Muon Facility (Eaton *et al.* 1994), where an E-field kicker is now used to distribute single muon pulses at 50Hz simultaneously to the three experimental areas, EMU, MuSR and DEVA, shown in Figure 11.

The kicker contains three electrodes, an outer, grounded pair and a thin central anode. The potential of the anode can be reduced from 32kV to zero in 100ns between the two muon pulses. Under normal working conditions, the first muon pulse experiences an electrostatic field on either side of the anode which gives rise to an equal division of the muon pulse and a right or left deflection of 3.8° to the septum magnet, situated 2.15m downstream of the kicker. Each deflected beam is deviated by a further 36.2° by the septum magnets to produce a total deflection between these beams of 80°. The second muon pulse experiences no electrostatic field and therefore is transmitted through the space between the septum magnets.

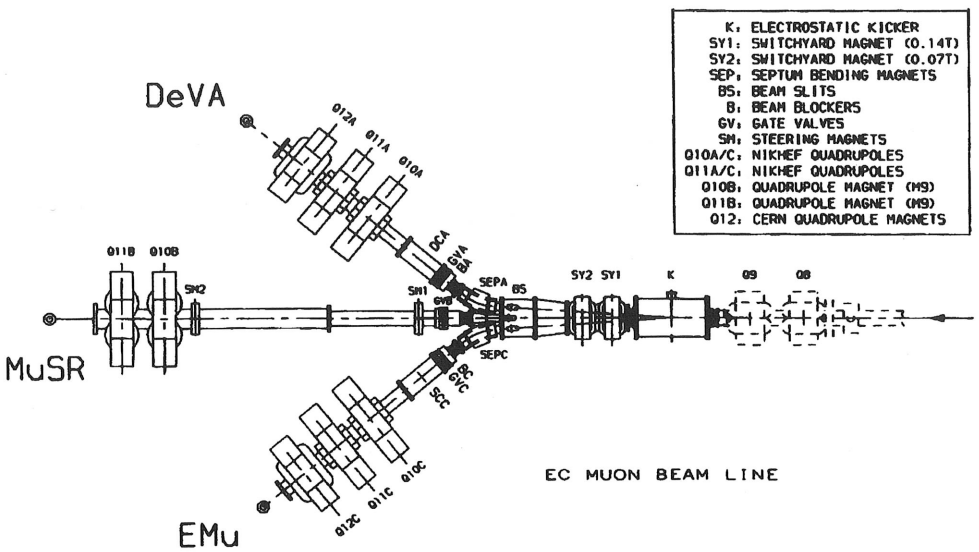

Figure 11. *Layout of the ISIS muon facility showing the locations of the E-field kicker K, the two septum magnets SEPA and SEPC and the three muon beamlines.*

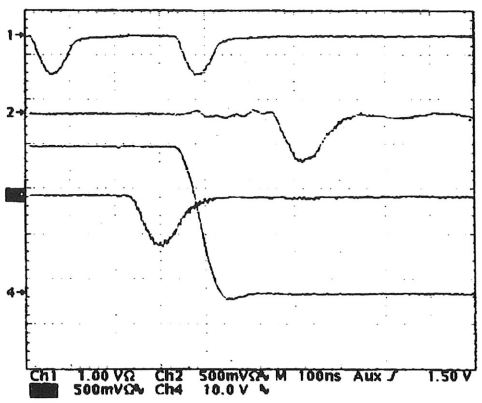

Figure 12. *Oscilloscope traces showing the action of the E-field kicker on the double pulses of muons.*

The action of this kicker on the double pulse structure can be seen in Figure 12. The top trace shows the pulses derived from a Cerenkov counter viewing the muon production target; and clearly shows the time structure of the two proton pulses on arrival at the target. The second and fourth traces show the MuSR and EMU muon pulses derived from scintillator rods mounted in horizontal collimators at the location BS in Figure 11. These show a clear separation of the two muon pulses into their septum magnets and hence into their respective experimental areas. A similar pulse (not shown) is transmitted to the DEVA area. The third trace shows the 32.5kV potential on the kicker as it ramps down between muon pulses.

The EC beamline spectrometers on MuSR and EMU

Figure 13 shows the DIZITAL instrument on the MuSR beam line, and the EC instrument on the EMU beam line. The technical specifications for these two instruments are given below. DIZITAL can be rotated for either transverse or longitudinal field geometries, whilst the EC instrument is dedicated to longitudinal geometry only. Both instruments require substantial segmentation of the positron detectors to minimise dead time corrections. The MuSR detector, for example, is composed of 32 segments, whilst EMU has 64 segments. In contrast to continuous sources, where coincidence techniques are used to introduce only one muon at a time to the sample, typically 10,000 muons per pulse are introduced simultaneously at ISIS. Consequently the effective instantaneous positron count rate is equivalent to the order of $5\times10^{9}\mathrm{s}^{-1}$.

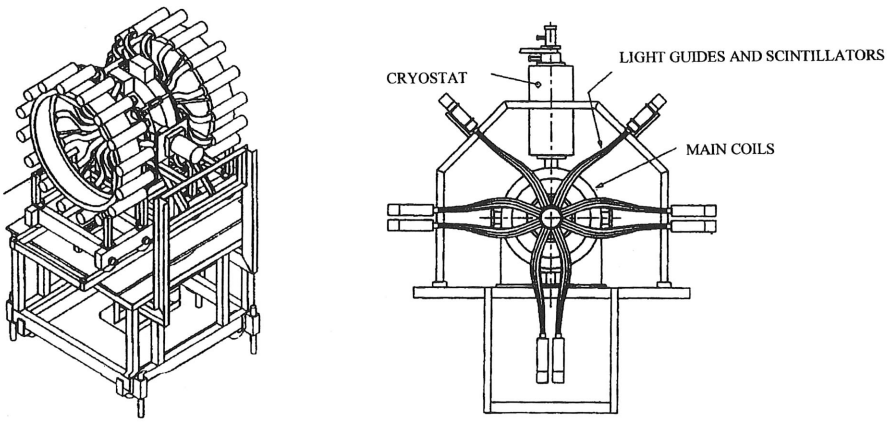

Figure 13. *(a) Example of a multidetector set-up for μSR: the DIZITAL spectrometer at ISIS. It has 16 forward and 16 backward detectors in the longitudinal configuration shown. Helmholtz coils produce a magnetic field along the cylindrical axis (arrow). It can also be used for transverse-field measurements. (b)The EMU μSR spectrometer at ISIS. Muons enter the apparatus perpendicular to the page.*

A particular advantage of the ISIS pulsed muon source is that once the muon pulse is introduced into the sample the beam is effectively switched off for a further 20ms. Therefore during the period over which the decay of the implanted muons is monitored the beam-borne backgrounds at the experiment are negligible. Muon decay processes can therefore be recorded over many (up to 15) muon lifetimes albeit with low counting statistics, as shown in Figure 14.

In contrast the intrinsic experimental background associated with those muons missing the sample and becoming implanted within the sample holder is generally lower on a continuous beam instrument, where it is relatively easy to define much smaller muon spots at the sample position. This is achieved using a scintillation counter with a hole of a diameter n appropriate to the sample size to veto any events associated with muons which do not pass through the hole. On pulsed source instruments, however, the spot size at the sample is determined by remote collimation (typically 1 $4\mathrm{cm}^2$), and a significant fraction

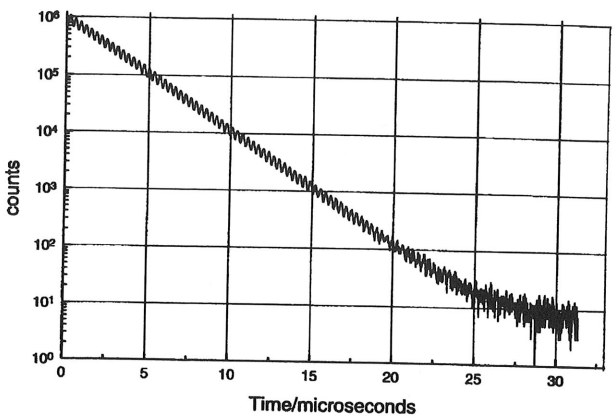

Figure 14. *Typical μSR transverse field spectrum at ISIS (2.2μs exponential removed) showing ability to trace muon behaviour up to 15τ_μ . The slight curvature beyond 25μs is due to the extremely small lifetime of the muon. Note that the intensity axis covers six orders of magnitude.*

of the incident muons associated with the beam penumbra may be implanted material surrounding the sample. The effects of such backgrounds can be minimised in transverse geometry experiments by surrounding the sample with haematite (Fe_20_3), which effectively depolarises all implanted muons and leaves a negligible background contribution. In longitudinal geometry the sample is surrounded by silver, in which muons are extremely mobile at all temperatures and do not depolarise, thereby contributing only a flat time and temperature independent background. There has also been some success in both transverse and longitudinal geometries using 'fly-by' sample mounts (Eaton *et al.* 1993). The technical specification for MuSR and EMU (revised in 1996) is given in the following table.

Beam

Production target	5, 7 or 10mm graphite
Momentum of μ^+	26.5MeV/c, 10% momentum bite
Pulse structure	single pulse 80ns FWHM
Contamination	$e^+/\mu^+ < 0.015$ (separator voltage> 70kV)
Beam size at focus	vertical 8mm (MuSR), 10mm (EMU)
(FWHM)	horizontal, adjustable 7–15mm (MuSR)
	10–27mm (EMU)
Total intensity	4×10^5 μ^+/s shared by the three areas
	(5mm target, ISIS current 180μA)
Polarisation	100%
Range	approx. 110mg/cm^2
Background	Histograms contain a constant background of about 10^{-5} times the count in the first bins
Data acquisition	Both instruments have 32 TDCs with time resolution settings of 8, 16, 24 or 32ns and each instrument is controlled by a VAX station 3200.

/continued

Sample Environment	
MuSR	Helmholtz coils (0–200mT) (transverse or longitudinal)
	Zero field compensation (<3μT)
	Closed cycle refrigerator (12–340K)
	Orange cryostat (2–300K)
	Dilution refrigerator (40mK–4.2K)
EMU	Helmholtz coils (0–450mT) (longitudinal only)
	Calibration coils (0–10mT) (transverse)
	Zero field compensation (< 3μT)
	Closed cycle refrigerator (12–340K)
	Oxford instruments cryostat (2–300K)
	Sorption cryostat (350mK–300K)

The EC beamline spectrometers on DEVA

The third beamline at ISIS, DEVA, is a development muon beamline for the exploration of "exotic" techniques and experiments. Currently these include RF techniques, fundamental muon physics, muon catalysed fusion and ultra cold muon research. As each of these topics is covered in detail in later chapters we shall briefly consider here just two of the current programmes on DEVA

RF techniques with muons

The possibility of adopting magnetic resonance methods for use with muons has long been realised (Garwin et al 1957 and Coffin *et al.* 1958). However, perhaps because of the short lifetime of the muon or, more probably, because of the simplicity and success of muon spin rotation and relaxation methods, there has not been a comparable exploitation of resonance techniques. Nevertheless, following the impressive demonstration of RF techniques at KEK (Katanka *et al.* 1982), a limited number of groups have used resonance methods to investigate topics which include chemical reactions (Sugai *et al.* 1992), final state determination (Azuma *et al.* 1986, Kreitzmann 1990), iron (Hampele *et al.* 1994) and semiconductors (Blazey *et al.* 1986 and Kreitzmann *et al.* to be published). Because of the short lifetime of the muon, the application of resonance techniques demand the generation of strong RF fields that, depending on the sample size and coil design, can require RF power levels of up to 2kW. At continuous muon sources the RF duty cycle can be as high as 50% (Kreitzmann 1990) with consequent experimental problems because of RF heating effects. Kitaoka et al (1982) have shown that this difficulty can easily be removed at a pulsed muon source where, by timing the RF field to be coincident with the muon pulse, an extremely low (~0.1% at ISIS) duty cycle can be achieved.

The motivation for developing resonance techniques at a pulsed muon source such as ISIS is high. For example, at a continuous muon source the maximum muon precession frequency that can be observed in a conventional transverse μSR experiment is restricted only by the time resolution of the detectors electronics. However at a pulsed source the maximum observable frequency is severely limited by the muon pulse width. Resonance techniques, and the 90° pulse method (Carne *et al.* 1984) in particular provide a method by which this limitation can be eliminated. This has been impressively demonstrated

by the recent work of Cottrell et al (1997) at ISIS. Using longitudinal geometry with an additional counter parallel to the initial muon polarisation, a 300ns long pulse of 23.5MHz RF was applied perpendicular to the static field of 17.2G, resulting in a 90° precession of the muon polarisation. The subsequent transverse field spectrum shown below was obtained for muonium in quartz. This observed muon precession frequency is well beyond that normally observable at ISIS using established μSR techniques. (See Figure 15.)

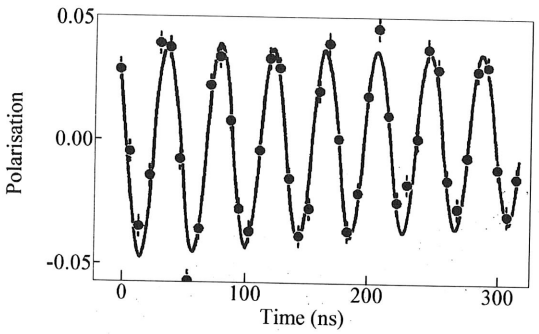

Figure 15. *Free precession of muonium in quartz after a 90° RF pulse at 23.5MHz.*

Working at a pulsed muon source has two additional advantages. Firstly, since all data collection is inherently time differential no experimental time penalty is involved in analysing data in this manner and secondly, because of the very low background between muon pulses, data can be collected to long times. It is likely that a future development of the RF technique will be the abandonment of digital counting techniques in favour of the implementation of the analogue detection systems pioneered at KEK by Yamazaki (1982) and already demonstrated at ISIS by the Stuttgart and Munich groups (1990).

Ultra-slow muons as a μSR probe for surfaces and thin films

The recent development work at PSI (Morenzoni *et al.* 1994) of the ultra slow muon moderation technique, first demonstrated at TRIUMF (Harshman *et al.* 1986), has shown that it is possible to thermally moderate surface muon beams with an efficiency of approximately 10^{-4} . For a moderator consisting of an aluminium substrate supporting a solid layer of a rare gas or nitrogen, the moderated muons emerge from the back of the moderator with energies peaked at 10eV and a polarisation of 87+3% and 80±20% in the respective cases of Ar and Kr solid layers. These results have indicated that the moderation process is relatively fast compared to any depolarisation mechanisms within the moderator and that the production of ultra slow muon beams for μSR is certainly feasible. Morenzoni (this volume) provides details of the work in progress at PSI. Following the success of these demonstrations a similar slow muon facility is currently under development on the DEVA beam line at ISIS. As with other μSR techniques, a pulsed muon beam has some advantages over a continuous source for ultra slow muon research, firstly because of the intrinsically low background, and secondly because a potentially intensity reducing incident muon monitor is not needed to provide the start pulse from which the muon decay is timed.

5.4 The Japanese RIKEN/RAL muon facility at ISIS

The second muon facility at ISIS is the RIKEN/RAL beam line, shown in Figure 16 and described by in the RIKEN-RAL Report (1997) and by Nagamine *et al.* (1993). This facility is based upon a decay muon channel and is currently by far the most intense source of pulsed muons in the world. The decay channel has three major components: a pion injection section near the production target, a 5.5m 5T superconducting solenoid in which pion decay takes place and a muon extraction section which transports the backward decay muons to the experimental area. The pion injector is designed to operate up to a maximum momentum of 250MeV/c pions and incorporates a pair of large aperture quadrupoles and a bending magnet to maximise the pion rate. The field generated by the superconducting solenoid is sufficiently high to capture all decay muons in tight spirals. The decay length λ_π in metres for pions of momentum p_π (MeV/c) is given by $\lambda_\pi = 0.055 p_\pi$. Thus for 100MeV/c pions $\lambda_\pi = 5.5$m.

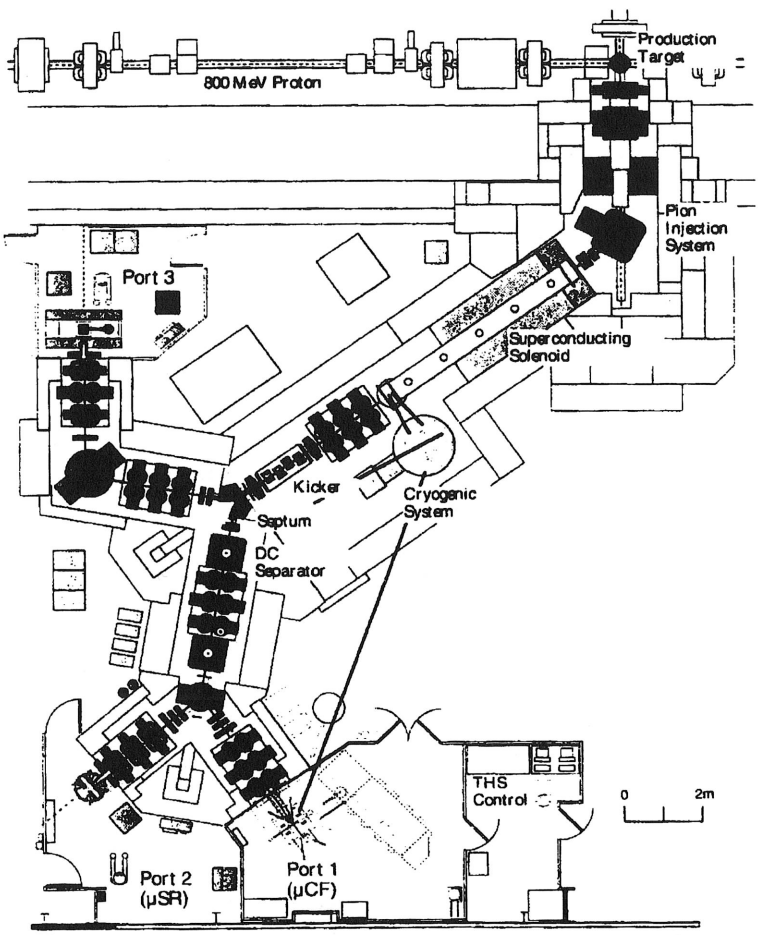

Figure 16. *The beamline and experimental ports of the RIKEN-RAL Muon Facility*

The exit aperture of the solenoid acts a source of either positive or negative muons depending on the charge sign of the input pions. The subsequent muon extraction system collects and transports those muons with a momentum corresponding to either forward or backward decays in the pion rest mass. By this method a high muon polarisation of (~80%) can be achieved. The muon extraction section has two unique features for a muon decay channel. Firstly a fast magnetic kicker (Figure 16) provides a magnetic field which rises rapidly to 0.02T between the two muon pulses, thereby separating the two pulses into two septum magnets and hence into two beam lines, such that two independent experimental areas can receive single muon pulses at 50Hz, as on the EC muon facility. The separation is possible up to a maximum muon momentum $p_\mu = 55$MeV/c. Above this momentum and up to $p_\mu = 120$MeV/c both pulses are directed to either of the two beamlines with steering magnets. The northward beam (to bottom of Figure 16), incorporates a switch yard magnet so that muons can be delivered to Port 1 or Port 2. The beamline incorporates two cross field electrostatic separators which eliminate the positron background in Port 1 or 2.

Experimental Areas of the RIKEN/RAL Muon Facility

- Port 1 of this facility is equipped with a highly sophisticated apparatus for research in muon catalysed nuclear fusion. This is a dedicated experiment which will be used over many years and which is already producing world class data of unprecedented quality. The permanence of this equipment, the high rates and very small backgrounds offers unique opportunities in this research field.
- Port 2 is the RIKEN μSR facility designated ARGUS, in which surface muons are used. Such use requires the whole beam line to be tuned to surface momentum 28MeV/c, and the design of the spectrometer, which incorporates a segmented detector consisting of 100 segments, allows unprecedented data acquisition rates approaching 10^8 events/hour.
- Port 3 is a general area for users to bring special apparatus for short stays, and is presently (1999) fully occupied with Japanese research on muonium production from hot foils and laser transitions in muonium.

5.5 Experimental muon science at ISIS

The experimental muon science programmes at ISIS have, in most cases, been extremely well suited to the characteristics of pulsed beam μSR. In many cases they have taken particular advantage of the extremely low beam-borne backgrounds to measure relaxation and rotation spectra in samples in which extreme motional narrowing or small internal field distributions lead to very low damping rates. Examples of such studies include flux lattice measurements in extreme type II superconductors (see for example, Lee, this volume) and spin fluctuations in itinerant magnets (Rainford, this volume). A recent independent review of the physics programme at ISIS noted the significance and importance of the following muon experiments:

- Observation of the critical slowing down of longitudinal spin fluctuations in itinerant 3d magnets; the crossover from itinerant to local moment behaviour (Cywinski and

Rainford 1994) and the first experimental demonstration of the direct correspondence of muon depolarisation rates with inelastic neutron scattering lineshapes in spin fluctuating compounds (Rainford et al 1992).

- The first unambiguous characterisation of the flux lattice melting and dimensional crossover in $Bi_{2.15}Sr_{1.85}CaCu_2O_{8+\delta}$. Precise determination of the flux distribution and hence penetration depth in a wide range of type II superconductors (Lee et al 1996 and references therein)
- Measurement of the internal filed distributions at mK temperatures in the fully organic ferromagnets p–NPNN and 3–QNNN (Blundell et al 1995).
- The first direct observation of the evolution of Kohlrausch relaxation in concentrated spin glasses above T_g (Campbell et al 1994).
- Diffusion and trapping of hydrogen in crystalline and amorphous materials by modelling the muon as a light isotope of hydrogen (Chow et al 1995).
- Measurement of the trapping and detrapping of electrons at muon (ie hydrogen) sites in semiconductors such as Ge and GaAs and muonium formation in Si and Ge. (see for example Cox and Lichti 1997 and references therein)
- Investigation of the superconducting state in the fullerenes and the molecular dynamics and anisotropic electron distribution in fullerenes by encapsulating atomic muonium in the fullerene cage. (Prassides 1993)
- Doppler-free laser spectroscopy for excitation of transitions between the 1S and 2S states in muonium enabling comparison with QED theory and precise determination of the mass of μ^+ (Jungmann et al 1991).

This list is by no means exclusive and many high profile experiments in physics, chemistry and materials have been reported over the past decade, many of which will be discussed in some detail in later chapters. It is also interesting to note that the physics review panel commented that "*the juxtaposition of muon and neutron facilities at ISIS has enabled the complementarity of μSR and neutron scattering to be explored and exploited in greater depth than ever before*". Indeed this juxtaposition has exposed a wider scientific community to the enormous potential of μSR and the cross fertilisation of muon and neutron beam studies, which is now also a feature of PSI following the commissioning of the SINQ neutron facility, is likely to enhance significantly the impact of both muon and neutron techniques in solid state science.

6 The future: muon facilities in the New Millennium

The three principal muon sources at PSI, TRIUMF and ISIS will continue to operate at their current specifications for perhaps the next 10–15 years, after which they will be approaching the end of their technically viable life. As the development of any major new accelerator-based facility takes well over a decade from conception to realisation it is vital that new world class muon facilities should already be under development. Fortunately one such source, the Japanese Hadron Facility (JHF) is currently being constructed while

a second, the European Spallation Source (ESS) , has been funded to the preliminary design stage. It is interesting that both the JHF and the ESS will emulate the remarkably successful ISIS model in juxtaposing muon and neutron beam facilities.

6.1 The Japanese hadron facility

This ambitious accelerator project is shown in Figure 17. This heart of this project is a 3GeV, 200μA proton beam generated from a 200MeV Linac and 3GeV fast cycling synchrotron complex. This beam is further accelerated in a 50GeV synchrotron to satisfy the needs of high energy physics. The principal advantages of JHF over ISIS is that although the proton currents are identical, the proton energy is almost four times higher. With double the number of protons/pulse at half the repetition rate, JHF will have significantly (5–10 times) higher instantaneous muon rates than ISIS. The JHF will have similar time structure to ISIS, so that the proposed muon facilities can incorporate several kicker magnets to multiplex many beams from a single production target. The proposed muon complex comprises surface and decay muon channels serving ten experimental areas.

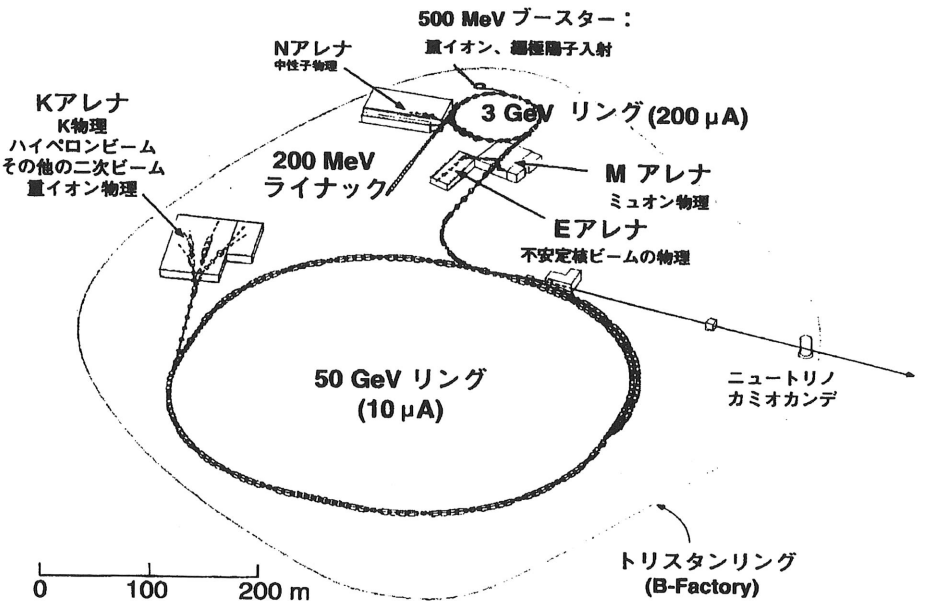

Figure 17. *Layout of the proposed Japanese Hadron Facility.*

6.2 The European Spallation Source

The proposed ESS (Gardner *et al.* 1995) is a third generation spallation neutron and muon source for Europe. It constitutes a major advance over the performance of ISIS.

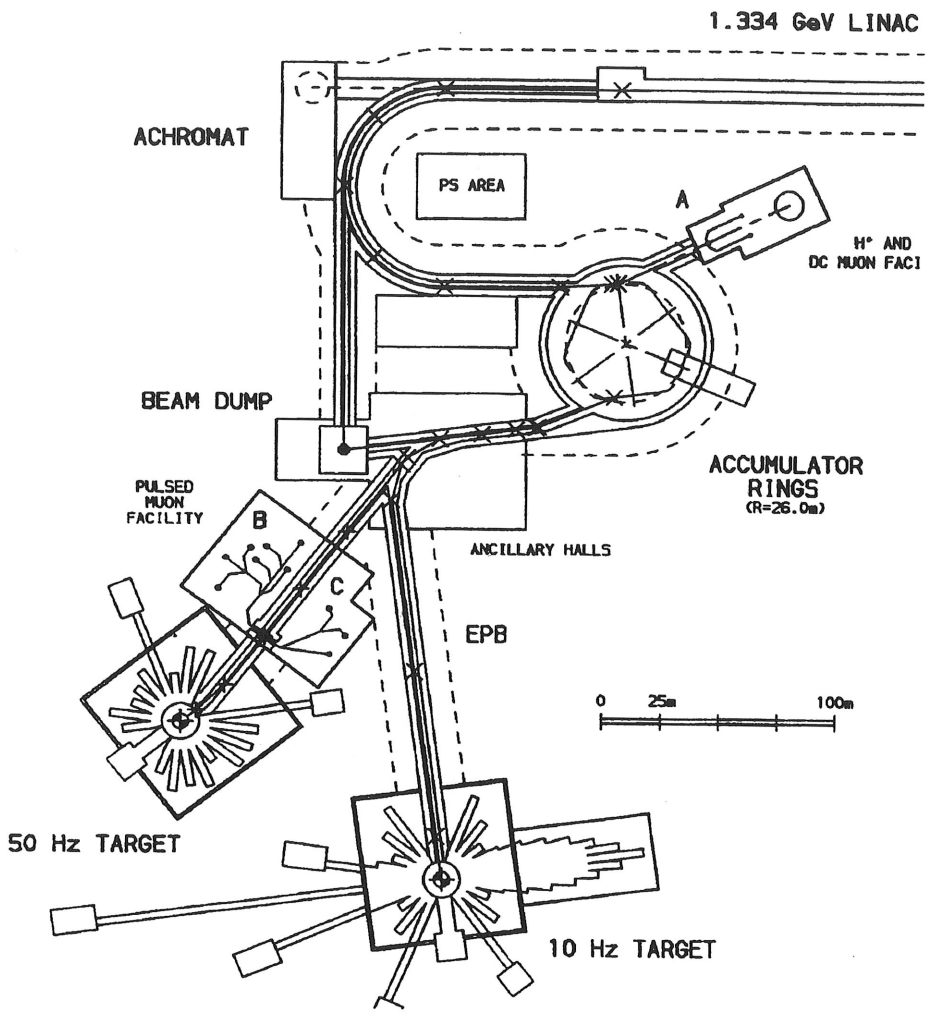

Figure 18. *The European Spallation Source: Layout of Accelerators and Beam Lines.*

The accelerator consists of a 1.334GeV Linac feeding continuous proton beams into an accumulator ring where bunching occurs to two proton bunches each 400ns long, within 1μsec total length. This 5MW proton beam is then extracted as in Figure 18 to a 50Hz 5MW or 10Hz 1MW target station for neutron production. The 50Hz neutron source will be approximately 30 times brighter than the ISIS source. In addition to neutrons the proposed ESS will also provide a high intensity source of muons. Because of the increased pulse length of the ESS proton pulse, fast kicker magnets can be used within the pulse itself as well as between pulses to produce six surface muon beams with single muon pulses of variable time width. Further decay beams and a high intensity pion/muon channel would be fed from the same target station, to give a total of thirteen beamlines with simultaneous single muon pulses (areas B and C in Figure 18). A further two beamlines also exist where muons could be switched on a longer time scale. The improvement of these beams over

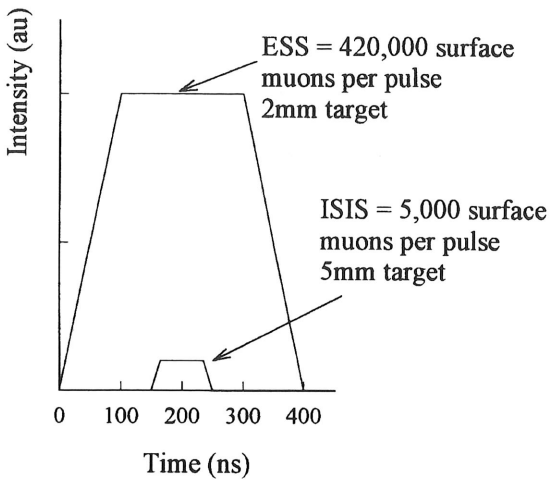

Figure 19. *Comparison between ESS and ISIS Surface Muon Intensities and Time Structure*

those at ISIS is clearly indicated by Figure 19, which compares the ESS muon pulse with that from ISIS. Such enormous increases would necessitate development of new detection techniques. It is also intended that a continuous muon facility will be based in Area A of Figure 18. Two surface muon channels would be competitive in intensity to PSI beams but would benefit from the smaller emittance of the ESS proton beam, allowing smaller final muon spots at the sample. The following table compares the three facilities.

Facility	Energy (GeV)	Protons/pulse	Repetition rate (Hz)	Current (μA)
ISIS	0.8	2.5×10^{13}	50	200
JHF	3.0	5.0×10^{13}	25	200
ESS	1.33	9.4×10^{14}	50	3770

Table 1. *A comparison between JHF, ESS and ISIS accelerators*

7 Conclusions

At ISIS we are fortunate to have what is currently the world's most powerful source of pulsed muons. This source complements admirably the world class continuous beam facilities at PSI and TRIUMF, As will be seen in the many examples of μSR science presented throughout this book, the character of the source often defines both the muon instrumentation and the experiments that are attempted at that source. It is also clear that muon science has developed as the sources themselves have developed. In this respect an extremely exciting prospect is that that the proposed third generation sources such as JHF and ESS are likely to lead muon science into new and as yet uncharted regions.

Acknowledgements

We would like to thank Chris Scott for allowing the use of some of his material for this report. We should also like, in a small way, to dedicate this report to our colleagues at RAL and in the international muon community who have contributed so much in realising the world's most powerful pulsed muon source at ISIS.

References

Abela R, Foroughi F and Renker D, 1991, Z Phys C **56** S240
Alexander G *et al.* 1967, Phys Rev **154** 1284
Alexander G *et al.* 1969, Nuclear Physics B **5** 1
Azuma T, Nishiyama K, Nagamine K, Ito Y, Tabata Y, 1986, Hyperfine Interactions **32** 837
Blazey K W, Estle T L, Rudaz S L, Holzschuh E, Kündig W and Patterson B D, 1986, Phys Rev B **34** 1422
Blundell S J *et al.* 1995, Europhysics Letters **31** 573
Borden A I, Carne A, Clarke-Gather M A, Eaton G H, Jones H J, Thomas G, Hartmann O and Sundquist T, 1990, Nucl Inst and Meth A **292** 21
Campbell I A, Schenck A, Herlach D, Gygax F N, Amato A, Cywinski R, Kilcoyne S H, 1994, Physical Review Letters **72** 1291
Carne A, Cox S F J, Eaton G H, De Renzi R, Scott C A, Stirling G C, 1984, Hyperfine Interactions **17-19** 945
Carrigan R A, 1968, Nuclear Physics B **6** 662
Chow *et al.* 1995, Physical Review B **51** 14762
Coffin T, Garwin R L, Penman S, Ledermann L, Sachs A M, 1958, Phys Rev **109** 973
Conversi M, Pancini E and Piccioni O, 1947, Phys Rev **71** 209
Cottrell S P, Scott C A and Hitti B, 1997, Hyperfine Interactions **106** 251
Cox S F J and Lichti R, 1997 Journal of Alloys and Compounds **253** 414
Cywinski R and Rainford B D, 1994, Hyperfine Interactions **85** 215
Daum M, Eaton G H, Frosch R, Hirschmann H, McCulloch J, Minehart R C and Steiner E, 1979, Phys Rev D **20** 2692
Eaton G H, Carne A, Cox S F J, Davies J D, De Renzi R, Hartmann O, Kratzer A, Ristori C, Scott C A, Stirling G C and Sundquist T, 1988, Nucl Inst and Meth A **269** 483
Eaton G H, Scott C A and Williams W G, 1993 Proc Int Workshop on Low Energy Muon Science LEMS '93 Los Alamos LA-12698-C
Eaton G H, Clarke-Gayther M A, Scott C A, Uden C N, Williams W G, 1994, Nucl Inst and Meth A **342** 319
Gardner I S K, Lengeler H and Rees G H, 1995, ESS Report ESS/P1/1995
Garwin, Ledermann and Weinrich, 1957, Phys Rev **105** 1415
Guzhavin V M *et al.* 1964, Soviet Phys JETP **19** 847
Hampele M, Herlach D, Kratzer A, Majer G, Major J, Raich H P, Roth R, Scott C A, Seeger A, Templ W, Blanz M, Cox S F J and Fürdere A, 1990, Hyperfine Interactions **65** 1082
Hampele M, Kratzer A, Maier K, Major J, Münch K H and Th Pfiz 1994, Hyperfine Interactions **87** 1043
Harshman D R, Warren J B, Beveridge J L, Kendall C R, Kiefl R F, Oram C J, Mills A P, Crane W S, Rupaal A S and Turner J H, 1986, Phys Rev Letters **56** 2850
Jones S E, 1986, Nature **321** 127
Jungmann K *et al.* 1991, Z Phys D 21 **21** 241
Katanka *et al.* 1982, Hyperfine Interactions **12** 51

Kreitzmann S R, 1990, Hyperfine Interactions **65** 1055
Kreitzmann S R, Hitti B, Lichti R, Estle, T L and Chow K H, 1999 (to be published)
Kunze P Z, 1933, Phys **83** 1
Lattes C M G, Muirhead H, Occhialini G P S and Powell C F, 1947, Nature **159** 694
Lee S L, Zimmermann P, Keller H, Warden M, Saviæ I M, Schauwecker R, Zech D, Cubitt R, Forgan E M, Kes P H, Li T W, Menovsky A A and Tarnawski Z 1993, Physical Review Letters **71** 3862
Maas F E *et al.* 1994, Physics Letters A **187** 247
Marshall G M Z, 1991, Phys C **56** S226
Morenzoni E, Kottmann F, Maden D, Matthias B, Meyberg M, Protscha Th, Wutzke T, Zimmermann V, 1994, Phys Rev Letters **72** 2793
Nagamine K, Matsuzaki T, Ishida K, Watanabe I, Kadono R, Eaton G H, Jones H J, Thomas G, Williams W G, 1993, Proc Int Workshop on Low Energy Muon Science Los Alamos LA-12698-C Los Alamos
Neddermeyer S H and Anderson C D, 1937, Phys Rev **51** 884
Particle Data Group, Phys Letters 75B1 (1978)
Piper A E, Bowen T, Kendall K R, 1976, Nucl Inst Meth **135** 39
Prassides K 1993, Physica Scripta T **49** 735
Rainford B D, Dakin S and Cywinski R, 1992, Journal of Magnetism and Magnetic Materials **104-107** 1257
RIKEN-RAL Muon Facility Report 1 (1997)
RIKEN-RAL Muon Facility Report (1995–1997) Volume 1 1997
Tanikawa K, Sakata S and Inoue T, 1946, Progr Theor Phys **1** 143
Scheck F, 1978, Phys Reports **44** 187
Schwarz W *et al.* 1995, IFEE transactions on Instrumentation and Measurement **44** 505
SIN Users Handbook 39 (1981) Sugai T, Kondow T, Matsushita A, Nishayama K, Nagamine K, 1992, Chemical Phys Letters **188** 100
Wu C S and Hughes V W, 1977, Muon Physics Academic Press, New York
Yamazaki T, Hayano R S, Kuno Y, Ohtake S and Nagae T, 1982, Nucl Inst and Methods **196** 289
Yukawa H, 1935, Proc Phys Math Soc Japan **17** 48